Desalination and Water Treatment
www.deswater.com

doi: 10.1080/19443994.2012.749191

51 (2013) 3371–3380
April

Taylor & Francis
Taylor & Francis Group

Cattail leaves as a novel biosorbent for the removal of malachite green from liquid phase: data analysis by non-linear technique

El-Khamsa Guechi, Oualid Hamdaoui*

Laboratory of Environmental Engineering, Department of Process Engineering, Faculty of Engineering, Badji Mokhtar-Annaba University, P.O. Box 12, Annaba 23000, Algeria
Tel./Fax: +213 38876560; emails: ohamdaoui@yahoo.fr; oualid.hamdaoui@univ-annaba.org

Received 22 December 2011; Accepted 4 November 2012

ABSTRACT

The ability of cattail (*Typha angustifolia*) leaves (CL) for the biosorption of malachite green (MG), a cationic dye, from aqueous solutions was investigated. Biosorption isotherm and kinetics of MG by CL were studied through a number of batch sorption experiments. The influence of operating conditions such as initial dye concentration, biosorbent dose, initial pH, stirring speed, temperature, ionic strength and biosorbent particle size on the removal of MG was investigated. Equilibrium data were fitted to the Langmuir, Freundlich, Redlich–Peterson and Sips isotherm models using non-linear regression technique. Experimental equilibrium data were best represented by the Redlich–Peterson and Sips isotherms, but the Redlich–Peterson model was better. Biosorption kinetics obtained at different initial concentrations were analysed using pseudo-first-order, pseudo-second-order and pseudo-*n*th order equations. The pseudo-*n*th order model fit the kinetic data well and was best than the pseudo-first- and pseudo-second-order equations. The order of biosorption reaction n was found to be between 1.27 and 1.93. The results revealed that the CL has the potential to be used as a biosorbent for the removal of MG from aqueous solutions.

Keywords: Biosorption; Malachite green; *Typha angustifolia*; Modelling; Non-linear technique

1. Introduction

Dye removal from industrial effluents has been the subject of great attention in the last few years. Approximately, 10–15% of the overall production of dyes is released into the environment, mainly via wastewater [1]. The presence of low concentration of dyes in the effluent streams is highly visible and undesirable, and it reduces the light penetration which leads to inhibiting photosynthesis and stringent restrictions on the organic content of industrial effluents.

In this work, the dye under consideration is malachite green (MG), which is a highly water soluble, basic dye of the triarylmethane class. MG is most widely used for colouring purpose, amongst all other dyes of its category [2]. This dye is widely used in the aquaculture industry worldwide as a biocide as well as in the silk, wool, cotton, leather, paper and acrylic industries as a dye. However, there are several reports describing its hazardous and carcinogenic effects [3,4]. Thus, keeping the hazardous nature and harmful effects in view, it was considered worthwhile to make systematic efforts to efficiently remove MG from wastewaters.

*Corresponding author.

Various conventional methods of colour removal from wastewater have been used. These include biological and physical–chemical process. However, these processes are difficult to handle and are not always effective and economical. Biosorption technology offers an efficient and cost-effective alternative compared to traditional chemical and physical remediation and decontamination methods. The major advantages of this method include: low cost, high efficiency, minimization of chemical or biological sludge, no additional nutrient requirement and possibility of effluent recovery [5,6]. A number of low-cost biosorbent have been studied in the literature for their capacity to remove MG from aqueous solutions [4,7–15].

Typha angustifolia (narrow-leaved cattail), a perennial macro-phyte, is characterized by its fast growing and high productivity [16–18]. *Typha angustifolia* belongs to the Typhaceae family. *Typha angustifolia* is an erect, perennial freshwater aquatic herb which can grow three or more metres in height. *Typha angustifolia* can be found in wetlands, sedge meadows, along slow moving streams, river banks and lake shores. The plant is found in areas of widely fluctuating water levels such as roadside ditches, reservoirs and other disturbed wet soil areas. Cattails (*Typha angustifolia*) flower in late May and June and sometimes later (up to late July) depending, perhaps, on soil and water temperatures as influenced by climate and litter in a stand. Fruits are mature in August and September [19]. The linear cattail leaves (CL) are thick, ribbon-like structures which have a spongy cross-section exhibiting air channels. Therefore, we attempt to use *Typha angustifolia* leaves as a cheap and renewable biosorbent for the removal of MG from aqueous solutions.

In this work, the potential of CL as novel biosorbent for the removal of MG from aqueous solution was investigated in batch process. Kinetic data and equilibrium isotherms were determined and analysed. The effects of various experimental parameters such as initial MG concentration, initial solution pH, stirring speed, biosorbent dose, temperature, particle size and ionic strength on MG biosorption were examined. The biosorption data were analysed and modelled using different models by non-linear regression method.

2. Materials and methods

2.1. Sorbate and biosorbent

The cationic dye (C.I. 42000; Basic Green 4), MG oxalate salt, (molecular formula $C_{52}H_{56}N_4O_{12}$, FW 929), was obtained from Merck and used without further purification. The calculated concentrations take into account the dye purity. Five hundred milligram per litre stock solution was prepared by dissolving the required amount of dye in distilled water. Working solutions of the desired concentrations were obtained by successive dilutions.

The collected leaves of cattail (*Typha angustifolia*) were washed with distilled water several times to remove dirt particles and water soluble materials. The washed materials were then completely dried in an oven at 50°C for five days. The dried leaves were then cut into small pieces, crushed and sieved to desired mesh size (1.25–2 mm). Finally, the obtained material was then dried in an air circulating oven at 50°C for seven days and stored in a desiccator until use.

2.2. Procedures

The initial concentration of MG solution was 50 mg L^{-1} for all experiments, except for those carried out to examine the effect of initial dye concentration. For dye removal kinetic experiments, the batch method was used because of its simplicity. About 0.25 g of biosorbent was contacted with 100 mL of dye solution in a sealed flask agitated vigorously by a magnetic stirrer using a water bath maintained at a constant temperature. The stirring speed was kept constant at 400 rpm, except for experiments carried out to investigate the effect of stirring speed. At predetermined intervals of time, samples of the mixture was withdrawn at suitable time intervals and analysed by a UV–Vis spectrophotometer (Jenway 6405) for the concentration of MG.

Sorption equilibrium experiments were carried out by adding a fixed amount of CL (0.25 g) into a number of sealed glass flasks containing a definite volume (100 mL in each case) of different initial concentrations (50–500 mg L^{-1}) of MG solution without changing pH. The flasks were placed in a thermostatic water bath in order to maintain a constant temperature (25, 35 or 45°C) and stirring was provided at 400 rpm to ensure equilibrium was reached. Samples of solutions were analysed for the remaining dye concentration with a UV–Vis spectrophotometer. The amount of sorption at equilibrium, q_e (mg g^{-1}), was calculated by:

$$q_e = \frac{(C_0 - C_e)V}{W} \quad (1)$$

where C_0 and C_e (mg L^{-1}) are the liquid phase concentrations of MG at initial and equilibrium time, respectively, V (L) is the volume of the solution and W (g) is the mass of used sorbent.

All the experiments were carried out in duplicate, and the mean values are presented. The maximum standard deviation was 3%.

3. Results and discussion

3.1. Effect of initial MG concentration

The effects of contact time and MG initial concentration on the biosorption uptake using CL at 25°C are shown in Fig. 1. The plots showed that the sorption of MG increase with time till it reached a constant value beyond which no more MG was further removed from the solution. The results revealed that the biosorption was fast at the initial stages of the contact period, and slowed down near equilibrium. The high sorption rate at the beginning of sorption was due to the sorption of dye molecules by the exterior surface of the biosorbent. When saturation was reached at the exterior surface, the MG molecules entered the pores of sorbent and were sorbed by the interior surface of the particles. The initial faster rates of sorption may also be attributed to the presence of large number of binding sites for sorption and the slower sorption rates at the end is due to the saturation of the binding sites and attainment of equilibrium. Similar behaviour was obtained for the sorption of MG by neem sawdust [10]. The necessary time to reach equilibrium is variable according to the initial concentration of dye: about 90 min for $C_0 = 5\,mg\,L^{-1}$, 120 min for $C_0 = 10\,mg\,L^{-1}$, 150 min for $20\,mg\,L^{-1}$, 180 for 30 and $40\,mg\,L^{-1}$ and 210 min for $50\,mg\,L^{-1}$.

From Fig. 1, it was also shown that the biosorption of MG increased with an increase in initial dye concentration and this confirmed strong chemical interactions between MG and biosorbent. This is due to increasing concentration gradient, which acts as increasing driving force to overcome all mass transfer resistances between the aqueous solution and solid phase [20].

3.2. Effet of initial solution pH

Fig. 2 shows the effect of initial pH on the biosorption of MG. It was observed that sorption of MG was strongly pH-dependent. MG is cationic dye, which exists in aqueous solution in the form of positively charged ions. As a charged species, the degree of its sorption by the biosorbent is primarily influenced by the surface charge on the sorbent, which in turn is influenced by the solution pH. As shown in Fig. 2, the equilibrium uptake of dye increased notably with raising the pH from 2 to 4. Above these levels, the sorption capacity did not change significantly up to pH 8. Similar trend was reported for sorption of MG by treated ginger waste [21]. The lower sorption of MG at acidic pH is due to the presence of excess H^+ ions that compete with the dye cation for sorption sites. As the pH of the system increases, the number of available positively charged sites decreases while the number of the negatively charged sites increases. The negatively charged sites favour the sorption of dye cation due to electrostatic attraction.

3.3. Effect of stirring speed

The effect of stirring speed ranging from 0 (without stirring) to 800 rpm on the sorption of MG by CL is shown in Fig. 3. The biosorption kinetics

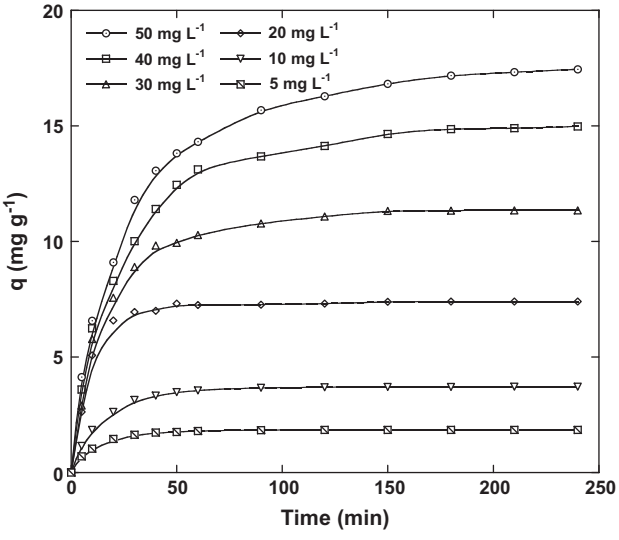

Fig. 1. Kinetics of MG biosorption by CL for various initial dye concentrations (conditions: sorbent dosage = 0.25 g $(100\,mL)^{-1}$; stirring speed = 400 rpm; $T = 25$°C; pH 4).

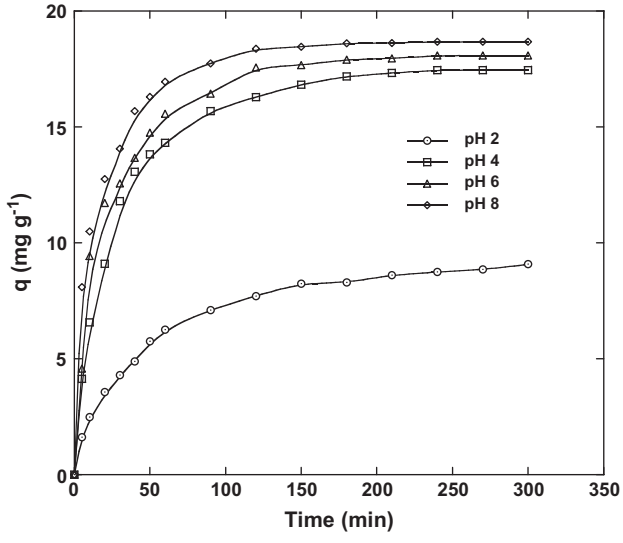

Fig. 2. Effect of initial pH on the biosorption of MG by CL (conditions: initial dye concentration = $50\,mg\,L^{-1}$; sorbent dosage = 0.25 g $(100\,mL)^{-1}$; stirring speed = 400 rpm; $T = 25$°C).

seems to be affected by the agitation speed in the range of 0–400 rpm. When increasing the agitation speed, the diffusion rate of dye molecules from the bulk liquid to the liquid boundary layer surrounding particles became higher because of an enhancement of turbulence and a decrease of the thickness of the liquid boundary layer. The insignificant effect of agitation for the range 400–800 rpm can be attributed to the strong turbulence and the very small thickness of the boundary layer around the biosorbent particles and an induction in the mobility of system.

3.4. Effect of biosorbent dosage

The effect of biosorbent dosage on the sorption of MG by CL is illustrated in Fig. 4. The amount of dye sorbed per unit mass of sorbent decreased with an increase in sorbent dosage. At higher biosorbent to sorbate concentration ratios, there is a very fast superficial sorption onto the sorbent surface that produces a lower solute concentration in the solution than when the biosorbent to solute concentration ratio is lower. This is because a fixed mass of biosorbent can only sorb a certain amount of dye. Therefore, the more the sorbent dosage, the larger the volume of effluent that a fixed mass of biosorbent can purify is. The decrease in amount of dye sorbed with an increasing sorbent mass is due to the split in the flux or the concentration gradient between solute concentration in the solution and the solute concentration in the surface of the sorbent. Thus, with an increasing sorbent mass, the amount of dye sorbed onto unit weight of sorbent gets reduced, thus causing a decrease in sorption capacity with an increasing sorbent dosage. Additionally, this decrease may be attributed to overlapping or aggregation of sorption sites resulting in decrease in total sorbent surface area available to dye molecules and an increase in diffusion path length.

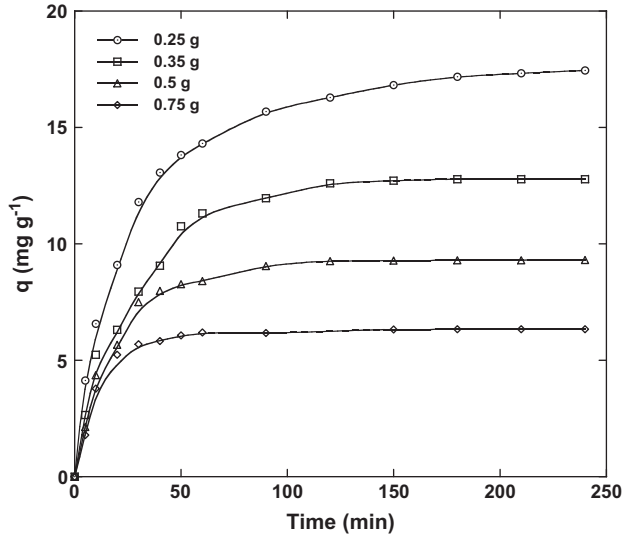

Fig. 4. Effect of biosorbent dosage on the biosorption of MG by CL (conditions: solution volume = 100 mL; initial dye concentration = 50 mg L^{-1}; stirring speed = 400 rpm; T = 25°C; pH 4).

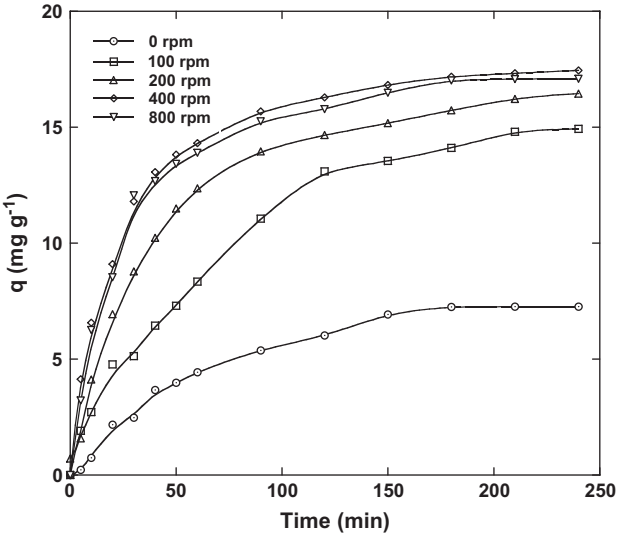

Fig. 3. Effect of stirring speed on the biosorption of MG by CL (conditions: initial dye concentration = 50 mg L^{-1}; sorbent dosage = 0.25 g $(100\,mL)^{-1}$; T = 25°C; pH 4).

3.5. Effect of temperature

Fig. 5 shows the effect of temperature on the biosorption of MG by CL. It was observed that the sorption uptake slightly increases with an increasing temperature. An increase in temperature increases the rate of diffusion of the sorbate molecules across the external boundary layer and within the internal pores of the biosorbent particle, due to decrease in the viscosity of the solution [22,23]. From the result, an increase in temperature from 25 to 45°C increased the sorption capacity from 17.45 to 18.84 mg g^{-1}, respectively, confirming the presence of strong chemical interactions between the dye and the material. This phenomenon indicates that the sorption process is endothermic in nature. This may be due to the mobility of molecules which increases generally with a rise in temperature, thereby facilitating the biosorption [5]. An increasing number of molecules may also acquire sufficient energy to undergo an interaction with active sites at the surface.

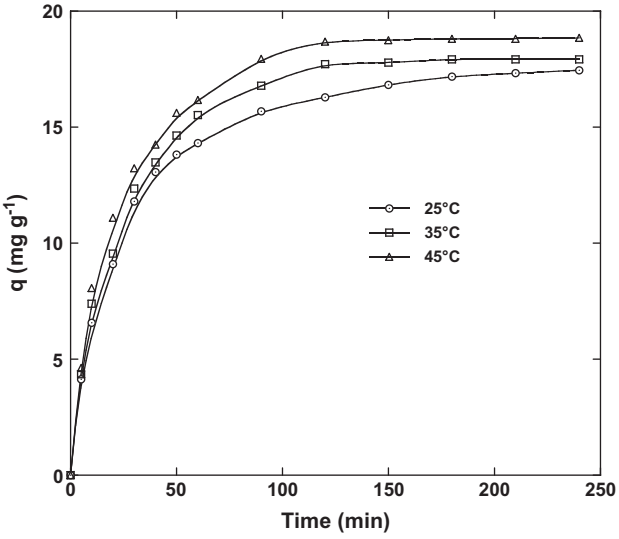

Fig. 5. Effect of temperature on the biosorption of MG by CL (conditions: initial dye concentration = 50 mg L^{-1}; sorbent dosage = 0.25 g $(100\,mL)^{-1}$; stirring speed = 400 rpm; pH 4).

3.6. Effect of particle size

The effect of biosorbent particle size on the MG removal was studied using three particle size ranges: 0.18–0.5, 0.5–1.25 and 1.25–2 mm. Fig. 6 shows the sorption kinetics of the dye at three different particle sizes. The biosorption rate and capacity increase with decreasing particle size of CL. Therefore, with a given mass of CL, smaller particle size would increase surface area availability hence the number of sites increased. Furthermore, access to the particle pores is facilitated when their size is small. It is also believed that the breaking up of large particles to form smaller ones opens some tiny sealed channels, which might then become available for sorption, and so the sorption by smaller particles is higher than that by larger particles. The relationship between the effective surface area of the sorbent particles and their sizes is that the effective surface area increases as the particle size decreases and as a consequence, the sorption capacity per unit mass of the sorbent increased. So the smaller biosorbent particle sizes for a given mass of biosorbent have more surface area and therefore the number of available sites is more.

3.7. Effect of ionic strength

The presence of salt leads to high ionic strength, which may significantly affect the performance of the biosorption process. Fig. 7 shows clearly that the variation of sodium chloride concentration exhibits a major effect on the extent of MG sorption. The reason for this is that Na^+ ions in the aqueous phase compete effectively with positively charged dye molecules for the same binding sites on the biosorbent surface. Additionally, ionic atmosphere may be progressively formed around MG molecules with increased sodium chloride concentration and results in the reduction of dye sorption on the tested biosorbent. Another reason is the influence of the great ionic strength on the

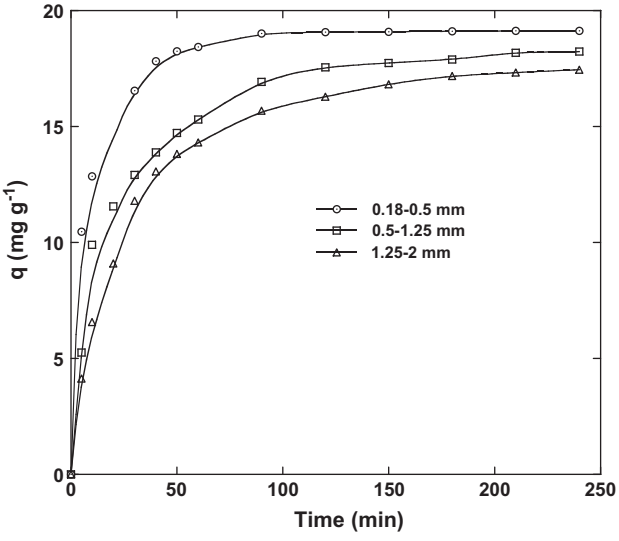

Fig. 6. Effect of biosorbent particle size on the biosorption of MG by CL (conditions: initial dye concentration = 50 mg L^{-1}; sorbent dosage = 0.25 g $(100\,mL)^{-1}$; stirring speed = 400 rpm; T = 25 °C; pH 4).

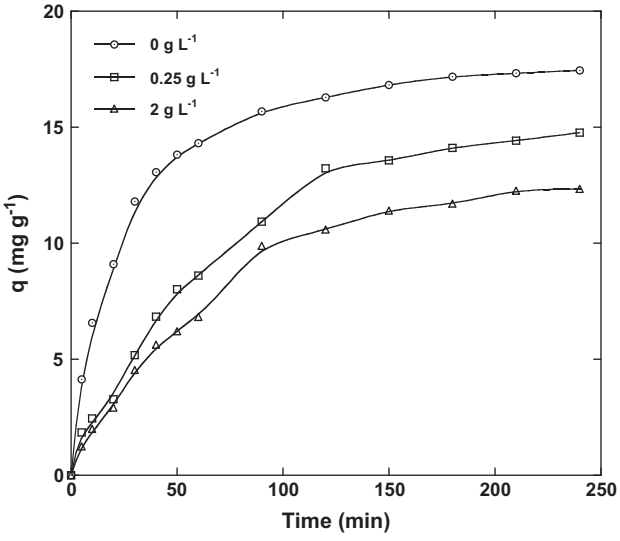

Fig. 7. Effect of salt (NaCl) concentration on the biosorption of MG by CL (conditions: initial dye concentration = 50 mg L^{-1}; sorbent dosage = 0.25 g $(100\,mL)^{-1}$; stirring speed = 400 rpm; T = 25 °C; pH 4).

activity coefficient of dye, which reduces its transfer to the sorbent surface [20].

3.8. Biosorption isotherms

The Langmuir model [24] assumes uniform energies of sorption onto the surface and no transmigration of sorbate in the plane of the surface. The Langmuir equation may be written as:

$$q_e = \frac{q_m b C_e}{1 + b C_e} \quad (2)$$

where q_e is the amount of solute sorbed per unit weight of sorbent at equilibrium ($mg\,g^{-1}$), C_e is the equilibrium concentration of the solute in the bulk solution ($mg\,L^{-1}$), q_m is the maximum sorption capacity ($mg\,g^{-1}$) and b is the constant related to the free energy of sorption ($L\,mg^{-1}$).

The Freundlich isotherm is an exponential equation and therefore, assumes that as the sorbate concentration increases, the concentration of sorbate on the sorbent surface also increases. The Freundlich equation [25] can be written as:

$$q_e = K_F C_e^{1/n} \quad (3)$$

where n is a constant indicative of the intensity of the sorption and K_F is a constant indicative of the relative sorption capacity of the sorbent ($mg^{1-\frac{1}{n}}L^{\frac{1}{n}}g^{-1}$).

The Redlich–Peterson isotherm [26] is an empirical isotherm incorporating three parameters. It combines elements from both the Langmuir and Freundlich equations, and the mechanism of sorption is a hybrid and does not follow ideal monolayer sorption:

$$q_e = \frac{A C_e}{1 + B C_e^{\beta}} \quad (4)$$

where A is the Redlich–Peterson isotherm constant ($L\,g^{-1}$), B is also a constant having unit of $(L\,mg^{-1})^{\beta}$, β is an exponent that lies between 0 and 1, C_e is the equilibrium liquid phase concentration of the sorbate ($mg\,L^{-1}$) and q_e is the equilibrium sorbate loading by the sorbent ($mg\,g^{-1}$).

Recognizing the problem of the continuing increase in the sorbed amount with an increase in concentration in the Freundlich equation, Sips [27] proposed an equation similar in form to the Freundlich equation, but it has a finite limit when the concentration is sufficiently high.

$$q_e = \frac{q_{m_S} K_S C_e^m}{1 + K_S C_e^m} \quad (5)$$

Table 1
Langmuir, Freundlich, Redlich–Peterson and Sips isotherm models constants and determination coefficients for the sorption of MG by CL at three different temperatures

Model	Parameters				
Langmuir	q_m ($mg\,g^{-1}$)	b ($L\,mg^{-1}$) $\times 10^3$	R^2	APE (%)	
25°C	72.25	81.69	0.968	11.70	
35°C	75.27	123.10	0.989	4.56	
45°C	76.70	170.57	0.985	7.46	
Freundlich	K_F ($mg^{1-\frac{1}{n}}L^{\frac{1}{n}}g^{-1}$)	n	R^2	APE (%)	
25°C	17.47	3.89	0.970	13.32	
35°C	21.85	4.37	0.972	11.61	
45°C	24.45	4.66	0.965	13.69	
Redlich–Peterson	A ($L\,g^{-1}$)	B $(L\,mg^{-1})^{\beta}$	β	R^2	APE (%)
25°C	9.88	0.29	0.86	0.980	10.03
35°C	13.16	0.28	0.91	0.996	4.09
45°C	17.43	0.34	0.92	0.992	6.68
Sips	q_{m_S} ($mg\,g^{-1}$)	K_S $((L\,mg^{-1})^m)$	m	R^2	APE (%)
25°C	95.78	0.13	0.56	0.977	10.88
35°C	83.53	0.17	0.70	0.993	5.29
45°C	83.07	0.22	0.73	0.988	7.86

where q_e is the sorbed amount at equilibrium ($mg\,g^{-1}$), C_e is the equilibrium concentration of the sorbate ($mg\,L^{-1}$), q_{ms} is the Sips maximum sorption capacity ($mg\,g^{-1}$), K_S is the Sips equilibrium constant $(L\,mg^{-1})^m$ and m is the exponent of Sips model.

In this work, four isotherm equations namely Langmuir, Freundlich, Redlich–Peterson and Sips were fitted to the experimental equilibrium data for MG at different temperatures by non-linear curve fitting analysis method using Microcal™ Origin® software. The results are shown in Table 1 and the modelled isotherms are plotted in Fig. 8.

The experimental values of q_e and C_e were analysed by non-linear curve fitting analysis in order to determine the models parameters and the isotherms were reconstituted using the determined values. The obtained curves showed the superposition of experimental results and the theoretical calculated points. The determination coefficients (R^2) showed the fit between experimental data and models while the average percentage errors (APEs) calculated according to Eq. (6) indicated the fit between the experimental and predicted values of the sorbed amount at equilibrium used for plotting isotherm curves.

$$\text{APE}\ (\%) = \frac{\sum_{i=1}^{N}\left|\frac{(q_e)_{\text{experimental}}-(q_e)_{\text{predicted}}}{(q_e)_{\text{experimental}}}\right|}{N}\times 100 \qquad (6)$$

where N the number of experimental data.

From Table 1 and Fig. 8, it was observed that the sorption equilibrium data were fitted well to the Redlich–Peterson model which combines the features of Langmuir and Freundlich models. Determination coefficients (R^2) and APEs for Redlich–Peterson model were determined in the range 0.980–0.996 and 4.09–10.03, respectively, for all the studied tempera-

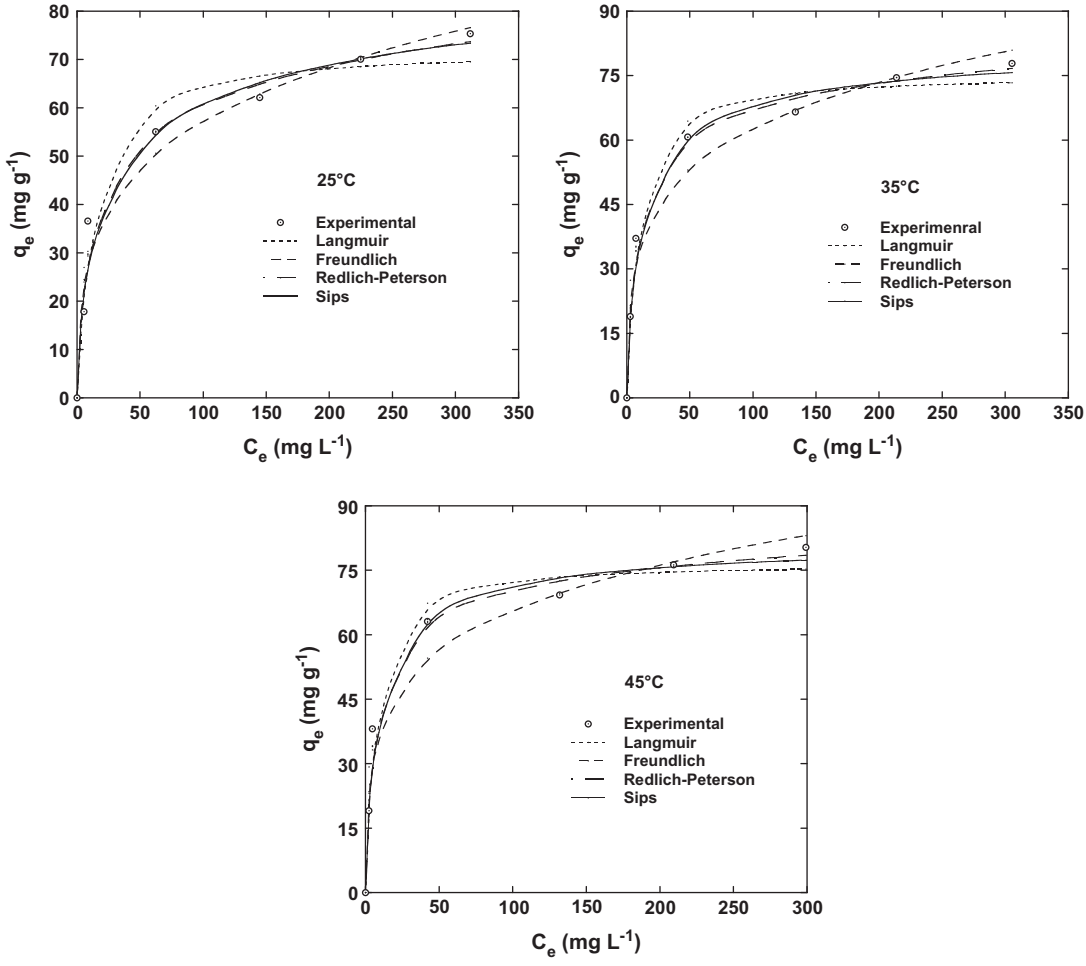

Fig. 8. Comparison between the experimental and predicted isotherms for the biosorption of MG by CL (conditions: initial dye concentration = 50–500 mg L^{-1}; sorbent dosage = 0.25 g (100 mL)$^{-1}$; stirring speed = 400 rpm; pH 4).

tures. Taking into account the APEs and determination coefficients, it was observed that both the Redlich–Peterson and Sips isotherms could well represent the experimental sorption data, but the Redlich–Peterson model was better.

The Langmuir isotherm exhibited acceptable coefficients of determination and APE values, but the values of maximum sorption capacity (Table 1) are lower than the experimental sorbed amounts at equilibrium corresponding to the plateaus of the sorption isotherms. Therefore, the Langmuir model is unable to describe the sorption isotherms of MG by CL. The Freundlich equation was not suitable for the description of equilibrium isotherms obtained at different temperatures because of the relatively higher values of APE.

3.9. Biosorption kinetics

The pseudo-first-order kinetic equation or the so-called Lagergren equation has the following formulation [28]:

$$\frac{dq}{dt} = k_1(q_e - q) \tag{7}$$

where k_1 is the pseudo-first-order rate constant (min^{-1}), q_e is the amount of sorbate sorbed at equilibrium ($mg\,g^{-1}$), q is the amount of sorbate on the surface of bisorbent at any time t ($mg\,g^{-1}$) and t is the time (min).

Özer [29] and Liu and Shen [30] have proposed to treat the pseudo-second-order equation as a special case of the more general rate law equation in which the order of sorption kinetics is not preset to a fixed value. Following Liu and Shen [30], the sorption reaction order is expressed with regard to the so-called effective concentration of the sorption sites available on the surface (which is a function of the amount sorbed at a given time and equilibrium). The simplicity of such an approach leads directly to both the pseudo-first- and the pseudo-second-order equations when the order of assumed reaction is preset to 1 and 2, respectively. The rate equation for this model can be written as follows:

$$\frac{dq}{dt} = k_n(q_e - q)^n \tag{8}$$

in which k_n is a constant and n is the sorption reaction order with regard to the effective concentration [30]. The n parameter value can be both integer and rational non-integer numbers.

If n equals 1, integrated form of Eq. (8) for the boundary conditions $q = 0$ when $t = 0$ and $q = q$ when $t = t$, will give Eq. (9).

$$q = q_e(1 - e^{-k_1 t}) \tag{9}$$

If n equals 2, after integrating Eq. (8) for the same condition, Blanchard's pseudo-second-order kinetic model equation will be obtained [31]

Table 2
Pseudo-first-order, pseudo-second-order and pseudo-*n*th order kinetic models constants and determination coefficients for the sorption of MG by CL

	5 mg L^{-1}	10 mg L^{-1}	20 mg L^{-1}	30 mg L^{-1}	40 mg L^{-1}	50 mg L^{-1}
Pseudo-first-order model						
k_1 (min^{-1}) $\times 10^3$	83.80	65.92	105.85	59.16	42.53	39.51
q_e ($mg\,g^{-1}$)	1.82	3.68	7.33	11.04	14.51	16.76
R^2	0.997	0.998	0.995	0.989	0.988	0.987
APE (%)	2.03	2.10	2.50	3.54	5.42	5.75
Pseudo-second-order model						
k_2 ($g\,mg^{-1}\,min^{-1}$) $\times 10^3$	65.97	24.30	21.08	6.93	3.58	2.78
q_e ($mg\,g^{-1}$)	1.97	4.02	7.85	12.18	16.26	18.93
R^2	0.990	0.990	0.973	0.994	0.997	0.999
APE (%)	3.61	3.97	5.87	3.28	1.91	1.45
Pseudo-nth order model						
k_n (min^{-1}) ($mg\,g^{-1}$)$^{1-n}$ $\times 10^3$	81.92	55.18	76.32	21.55	6.63	3.45
n	1.27	1.23	1.22	1.51	1.77	1.93
q_e ($mg\,g^{-1}$)	1.85	3.72	7.40	11.49	15.75	18.72
R^2	0.999	0.999	0.993	0.997	0.998	0.999
APE (%)	0.83	0.65	2.83	2.31	1.94	1.53

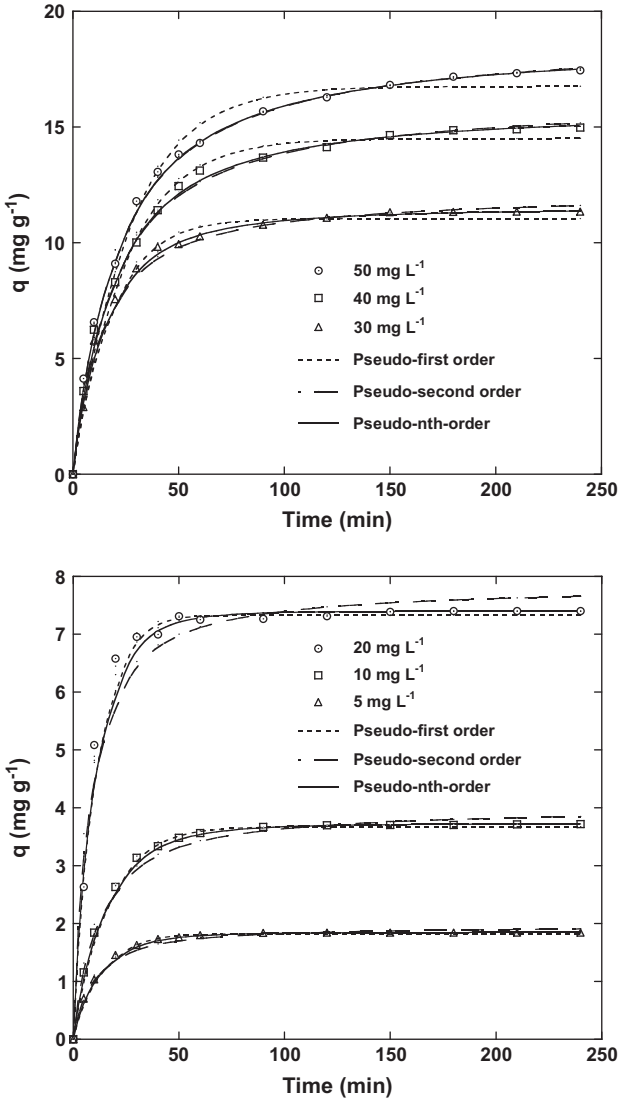

Fig. 9. Comparison of experimental and predicted kinetics for the biosorption of MG by CL at various initial dye concentrations.

$$q = \frac{k_2 q_e^2 t}{1 + k_2 q_e t} \tag{10}$$

Eq. (8) was integrated for pseudo-*n*th order and following non-linear equation was obtained.

$$q = q_e - [(n-1)k_n t + q_e^{(1-n)}]^{\frac{1}{1-n}} \tag{11}$$

The kinetics of the biosorption process was analysed using the pseudo-first-order, pseudo-second-order and pseudo-*n*th order equations to model the kinetics of MG sorption by CL using non-linear fitting analysis method using Microcal™ Origin® software.

Fig. 9 shows experimental data and the predicted curves for the biosorption of MG by CL using non-linear method for the three used models. Table 2 shows the pseudo-first-order, pseudo-second-order and pseudo-*n*th order kinetic parameters for different initial concentrations of MG obtained by utilizing the non-linear regression analysis method. From Fig. 9 and Table 1, it seems that the pseudo-*n*th order model fit the experimental data well and was best than the pseudo-first- and pseudo-second-order equations because of the low APE values and good coefficients of determination. The order of sorption reaction n was found to be between 1.27 and 1.93. For initial dye concentrations of 40 and 50 mg L^{-1}, taking into account the APEs and determination coefficients, it was observed that both the pseudo-*n*th order and pseudo-second-order equations could well represent the experimental sorption data, but the pseudo-second-order model was slightly better. The suitability of the pseudo-second-order equation to fit the data at higher initial dye concentrations was confirmed by the exponent value of the pseudo-*n*th order model, which was equal to 1.77 and 1.93 for initial dye concentration of 40 and 50 mg L^{-1}, respectively.

For the pseudo-first-order model, although the coefficient of determination values are reasonably high, the calculated sorption capacity values obtained from this kinetic model do not give reasonable values compared with experimental sorption capacity. This finding suggested that the sorption process does not follow the pseudo-first-order sorption rate expression of Lagergren.

4. Conclusion

The sorption of MG from aqueous solution using CL was investigated in batch mode. The effects of experimental parameters such as initial dye concentration, biosorbent dose, initial pH, stirring speed, temperature, ionic strength, biosorbent particle size on dye biosorption were studied. Initial dye concentration, sorbent dose, initial pH, stirring speed, ionic strength and biosorbent particle size were found to have an influence on the biosorption efficiency. However, temperature showed a restricted effect on the removal kinetics. The equilibrium data were analysed by non-linear curve fitting analysis method using the Langmuir, Freundlich, Redlich–Peterson and Sips isotherms. The data were better described by the Redlich–Peterson model. Kinetic data were tested using the pseudo-first-order, pseudo-second-order and pseudo-*n*th order kinetic models. Kinetic data were

adequately fitted by the pseudo-*n*th order model and was best than the pseudo-first-order and pseudo-second-order equations. CL used in this work is freely and abundantly available, do not require an additional pretreatment step such as activation before applications and possess high sorption capacity for MG. Therefore, the sorbent is expected to be economically feasible for removal of MG dye from aqueous solutions.

Acknowledgements

The financial support by the General Directorate for Scientific Research and Technological Development (PNR project No. 4/D/25) and the Ministry of Higher Education and Scientific Research of Algeria (projects Nos. J0101120090018 and J0101120120098) is greatly acknowledged.

References

[1] H. Zollinger, Color Chemistry: Synthesis, Properties and Application of Organic Dyes and Pigments, VCH Publishers, New York, NY, 2004.
[2] G. Crini, H.N. Peindy, F. Gimbert, C. Robert, Removal of C.I. Basic Green 4 (Malachite Green) from aqueous solutions by adsorption using cyclodextrin-based adsorbent: Kinetic and equilibrium studies, Sep. Purif. Technol. 53 (2007) 97–110.
[3] A. Srivastava, R. Sinha, D. Roy, Toxicological effects of malachite green, Aquat. Toxicol. 66 (2004) 319–329.
[4] B.H. Hameed, M.I. El-Khaiary, Batch removal of malachite green from aqueous solutions by adsorption on oil palm trunk fibre: Equilibrium isotherms and kinetic studies, J. Hazard. Mater. 154 (2008) 237–244.
[5] N. Nasuha, B.H. Hameed, A.T. Mohd Din, Rejected tea as a potential low-cost adsorbent for the removal of methylene blue, J. Hazard. Mater. 175 (2010) 126–132.
[6] D. Sud, G. Mahajan, M.P. Kaur, Agricultural waste material as potential adsorbent for sequestering heavy metal ions from aqueous solutions—a review, Bioresour. Technol. 99 (2008) 6017–6027.
[7] M.-H. Baek, C.O. Ijagbemi, S.-J. O, D.-S. Kim, Removal of Malachite Green from aqueous solution using degreased coffee bean, J. Hazard. Mater. 176 (2010) 820–828.
[8] Z. Bekçi, Y. Seki, L. Cavas, Removal of malachite green by using an invasive marine alga Caulerpa racemosa var. cylindracea, J. Hazard. Mater. 161 (2009) 1454–1460.
[9] O. Hamdaoui, M. Chiha, E. Naffrechoux, Ultrasound-assisted removal of malachite green from aqueous solution by dead pine needles, Ultrason. Sonochem. 15 (2008) 799–807.
[10] S.D. Khattri, M.K. Singh, Removal of malachite green from dye wastewater using neem sawdust by adsorption, J. Hazard. Mater. 167 (2009) 1089–1094.
[11] K. Mittal, Adsorption kinetics of removal of a toxic dye, Malachite Green, from wastewater by using hen feathers, J. Hazard. Mater. 133 (2006) 196–202.
[12] C. Pradeep Sekhar, S. Kalidhasan, V. Rajesh, N. Rajesh, Biopolymer adsorbent for the removal of malachite green from aqueous solution, Chemosphere 77 (2009) 842–847.
[13] G.H. Sonawane, V.S. Shrivastava, Kinetics of decolourization of malachite green from aqueous medium by maize cob (Zea maize): An agricultural solid waste, Desalination 247 (2009) 430–441.
[14] K. Vasanth Kumar, V. Ramamurthi, S. Sivanesan, Biosorption of malachite green, a cationic dye onto Pithophora sp., a fresh water algae, Dyes Pig. 69 (2006) 102–107.
[15] G. Crini, Non-conventional low-cost adsorbents for dye removal: A review, Bioresour. Technol. 97 (2006) 1061–1085.
[16] D. Demirezen, A. Aksoy, Accumulation of heavy metals in *Typha angustifolia* (L.) and *Potamogeton pectinatus* (L.) living in Sultan Marsh (Kayseri, Turkey), Chemosphere 56 (2004) 685–696.
[17] T. Panich-Pat, P. Pokethitiyook, M. Kruatrachue, E.S. Upatham, P. Srinives, G.R. Lanza, Removal of lead from contaminated soils by *Typha angustifolia*, Water Air Soil Pollut. 155 (2004) 159–171.
[18] J. Dong, F.B. Wu, R.G. Huang, G.P. Zang, A chromium-tolerant plant growing in Cr-contaminated land, Int. J. Phytoremediat. 9 (2007) 167–179.
[19] P.A. Keddy, T.H. Ellis, Seedling recruitment of 11 wetland plant species along a water level gradient: Shared or distinct responses? Can. J. Bot. 63 (1985) 1876–1879.
[20] O. Hamdaoui, F. Saoudi, M. Chiha, E. Naffrechoux, Sorption of malachite green by a novel sorbent, dead leaves of plane tree: Equilibrium and kinetic modeling, Chem. Eng. J. 143 (2008) 73–84.
[21] R. Ahmad, R. Kumar, Adsorption studies of hazardous malachite green onto treated ginger waste, J. Environ. Manage. 91 (2010) 1032–1038.
[22] O. Hamdaoui, F. Saoudi, M. Chiha, Utilization of an agricultural waste material, melon (Cucumis melo L.) peel, as a sorbent for the removal of cadmium from aqueous phase, Desalin. Water Treat. 21 (2010) 228–237.
[23] S. Boutemedjet, O. Hamdaoui, Sorption of malachite green by eucalyptus bark as a non-conventional low-cost biosorbent, Desalin. Water Treat. 8 (2009) 201–210.
[24] I. Langmuir, The constitution and fundamental properties of solids and liquids, J. Am. Chem. Soc. 38 (1916) 2221–2295.
[25] H.M.F. Freundlich, Über die adsorption in lösungen, Z. Phys. Chem. 57 (1906) 385–470.
[26] O. Redlich, D.L. Peterson, A useful adsorption isotherm, J. Phys. Chem. 63 (1959) 1024–1026.
[27] R. Sips, On the structure of a catalyst surface, J. Chem. Phys. 16 (1948) 490–495.
[28] S. Lagergren, About the theory of so-called adsorption of soluble substances, K. Sven. Vetenskapsakad. Handl. 24 (1898) 1–39.
[29] A. Özer, Removal of Pb(II) ions from aqueous solutions by sulphuric acid-treated wheat bran, J. Hazard. Mater. 141 (2007) 753–761.
[30] Y. Liu, L. Shen, A general rate law equation for biosorption, Biochem. Eng. J. 38 (2008) 390–394.
[31] G. Blanchard, M. Maunaye, G. Martin, Removal of heavy metals from waters by means of natural zeolites, Water Res. 18 (1984) 1501–1507.